Smart Mater. Struct. 6 (1997) 102–105. Printed in the UK PII: S0964-1726(97)79317-0

A new electromechanical effect in discontinuous-filament elastomer-matrix composites

Xiaoping Shui and D D L Chung

Composite Materials Research Laboratory, State University of New York at Buffalo, Buffalo, NY 14260-4400, USA

Received 17 September 1996, accepted for publication 23 October 1996

Abstract. A new electromechanical effect in which the volume electrical resistivity decreased upon tensile loading and increased upon unloading was observed in elastomer- (silicone-) matrix composites with a discontinuous and randomly oriented nickel filament filler. The effect is probably due to the increase in filament alignment upon tensile loading. It allows tensile strain sensing. However, filament–matrix interface degradation caused the resistivity to increase irreversibly and the electromechanical effect to diminish as cycling progressed beyond the first 10–30 cycles.

1. Introduction

Electromechanical effects in which the volume electrical resistivity of a material changes upon deformation provide the scientific foundation for many strain sensors. Piezoresistivity, in which the resistivity increases under tension and decreases upon compression due to the change in separation between adjacent conducting units in a composite material [1–4], is an example of an electromechanical effect. In order for the sensor to be used more than once, the effect must be reversible. This paper is concerned with a new electromechanical effect in which the resistivity decreases reversibly upon tensile loading. The effect is opposite to piezoresistivity and is probably due to the change in the degree of conducting unit alignment in a composite material.

2. Experimental methods

The silicone used was silicone rubber RTV615 (two parts) from General Electric Co. The specific gravity was 0.99. The nickel filaments used were the same as those in [5]. Their diameter was 0.4 μm; their length was greater than 100 μm. They were not straight, but resembled cotton wool. Each nickel filament contained a carbon core of diameter 0.1 μm, so the filament contained 94 vol.% nickel and 6 vol.% carbon.

Composite fabrication was carried out by (i) mixing part A (resin) and part B (curing agent) of RTV615 at a weight ratio of 10:1, (ii) adding nickel filaments and mixing; (iii) pressing in a mold at 400 psi (2.8 MPa) and room temperature for 12 h, and (iv) while keeping the pressure at 400 psi, heating at 60–70 °C for 2 h.

The electrical resistance R was measured using the four-probe method while cyclic tension–compression was applied. The strain amplitude was much higher under tension than under compression. Copper clips were used for electrical contacts. The four probes consist of two outer current probes and two inner voltage probes. The resistance R refers to the sample resistance between the inner probes. The distance between the inner probes was 20 mm. The fractional increase in R is approximately equal to the fractional increase in resistivity ρ only at small strains (less than 1.5%), as found theoretically by assuming that the sample volume remains constant upon tension. The samples were in the shape of a dog bone, with thickness 2.8 mm and size shown in figure 1, as obtained by cutting using a die (ASTM D412, die D). The resistance was measured along the stress axis. The current (DC) used was 0.5–1.0 mA; the voltage used was 2.0–2.4 V. The displacement rate was 1.0 mm min^{-1}. Testing was conducted by using a screw-action materials testing system (Sintech 2/D) and wedge-action grips for gripping the sample. Tensile testing (ASTM D412-87) was similarly performed, except that R was not measured.

The volume electrical resistivity of the composites was measured by the four-probe method, using silver paint as electrical contacts. The samples were of size 100 mm × 5 mm × 3 mm, such that the current was along the longest dimension and the inner (voltage) probes were 50 mm apart in this direction.

3. Results and discussion

Figure 2 shows the strain (figure 2(a)), stress (figure 2(b)) and fractional resistance increase ($\Delta R/R_0$) obtained

0964-1726/97/010102+04$19.50

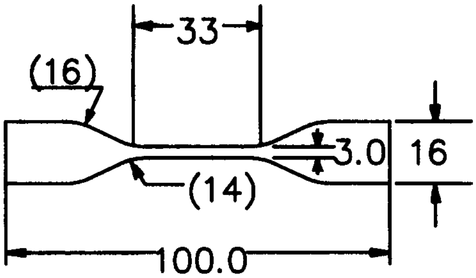

Figure 1. The sample configuration for electromechanical and mechanical testing. All dimensions are in millimeters. Numbers in parentheses refer to the radius of curvature.

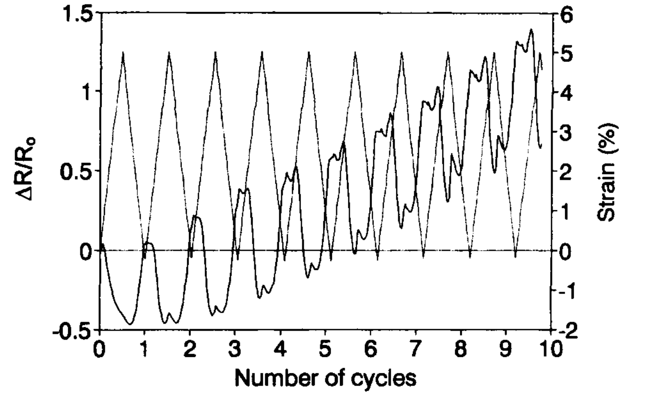

(*a*)

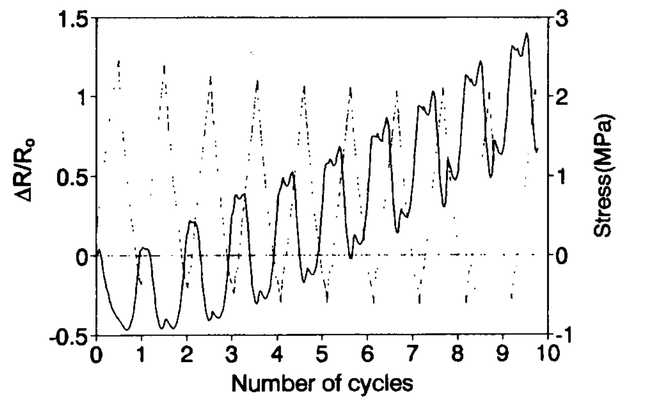

(*b*)

Figure 2. The variation of $\Delta R/R_0$ (solid line), strain (dashed line, (*a*)) and stress (dashed line, (*b*)) with time during cyclic loading (mostly tensile) up to ten cycles for a composite containing 7 vol.% nickel filaments.

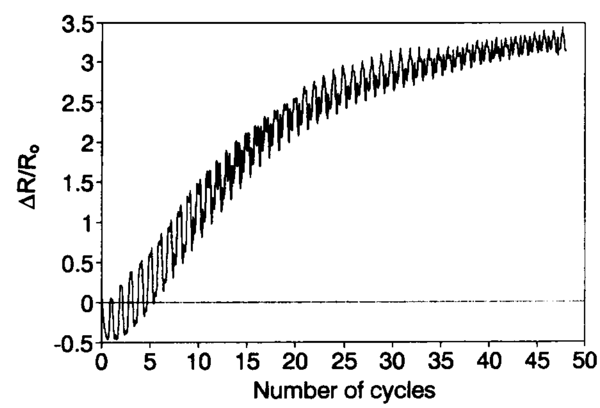

Figure 3. The variation of $\Delta R/R_0$ during cyclic loading up to 48 strain cycles for the sample and cyclic loading conditions of figure 2.

simultaneously during cyclic tension–compression up to ten cycles for a composite with 7 vol.% nickel filaments. The strain amplitude was 5% under tension and 0.2% under compression. The resistance decreased upon tensile loading in every cycle and increased upon tensile unloading in every cycle. This effect cannot be due to dimensional changes, as dimensional changes under tension would have increased the resistance and dimensional changes under compression would have decreased the resistance. The effect cannot be due to piezoresistivity, which would have caused the resistance to increase under tension and decrease under compression. Nor can this phenomenon be due to filament–matrix bond degradation, as this degradation would have caused the resistance to increase upon tension and is not reversible in any case. As the nickel filaments had a randomly oriented and bent morphology resembling cotton wool and the matrix was elastomeric, the filaments most probably increased in their degree of alignment when the composite was under tension. The increase in filament alignment would cause the resistance to decrease. Hence, the observed phenomenon is tentatively attributed to the increase in the degree of filament alignment along the stress axis upon tension. The small change in resistance that occurred whenever the stress changed direction and that increased in magnitude with increasing cycle number is probably an artifact resulting from the imperfect gripping of the elastomeric sample under cyclic loading. The imperfect gripping probably caused some buckling of the sample during compression. During the first seven cycles, the maximum value of $\Delta R/R_0$ in a cycle increased as cycling progressed, so that the amplitude of $\Delta R/R_0$ increased. The upshift of the peak $\Delta R/R_0$ was irreversible and was probably due to degradation of the filament–matrix bonding; it was not due to filament breakage because the tensile modulus (as indicated by the slope of the stress–strain curve) did not change upon cycling. The increase in the $\Delta R/R_0$ amplitude during the first seven cycles is probably due to the increase in the degree of fiber alignment upon cycling. As cycling progressed beyond about the tenth cycle, the amplitude of $\Delta R/R_0$ decreased, as shown in figure 3 up to 48 cycles. For all cycles beyond the first cycle, both the minimum and maximum values of $\Delta R/R_0$ in a cycle increased with increasing cycle number, though these changes with cycle number leveled off gradually as cycling progressed. These changes in minimum and maximum $\Delta R/R_0$ and the decrease in $\Delta R/R_0$ amplitude beyond the tenth cycle are attributed to filament–matrix interface degradation, which increased R irreversibly and decreased the tendency for the filaments to align upon tension.

Figure 4 shows $\Delta R/R_0$ obtained during cyclic tension–compression up to 30 cycles for the same composite as in figures 2 and 3, but, in contrast to figures 2 and 3, the strain amplitude was 20% under tension and 5% under

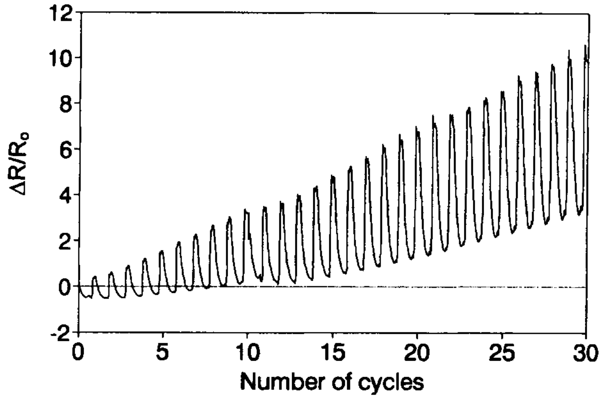

Figure 4. The variation of $\Delta R/R_0$ during cyclic loading up to 30 strain cycles for the sample of figures 2 and 3 but at a tensile strain amplitude of 20%.

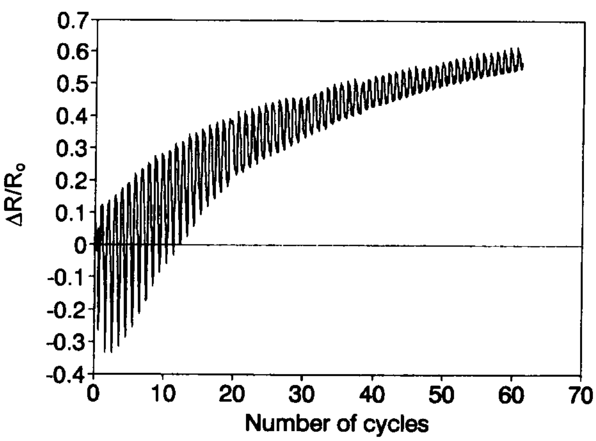

Figure 5. The variation of $\Delta R/R_0$ during cyclic loading up to 60 strain cycles for a composite with 10 vol.% nickel filaments at a tensile strain amplitude of 5%.

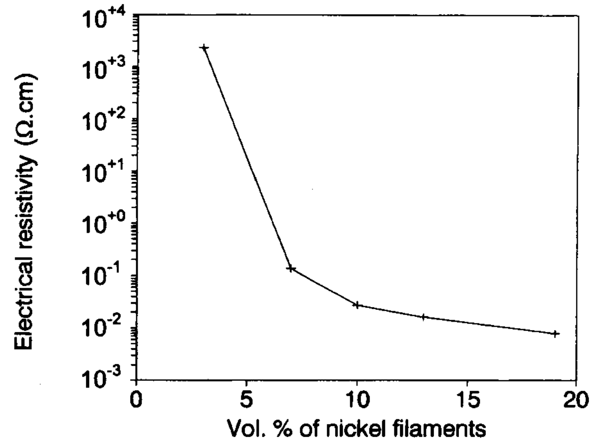

Figure 6. The variation of the volume electrical resistivity with nickel filament volume fraction at no load and without prior loading.

compression. The $\Delta R/R_0$ amplitude and minimum and maximum $\Delta R/R_0$ increased with increasing cycle number, at least up to the 30th cycle. The increase in $\Delta R/R_0$ amplitude was probably due to the increase in degree of fiber alignment as cycling progressed; the effect is more pronounced than that in figure 2 due to the higher tensile strain amplitude. The increase in minimum and maximum $\Delta R/R_0$ was probably due to filament–matrix interface degradation as cycling progressed.

Figure 5 shows $\Delta R/R_0$ obtained during cyclic tension–compression up to 60 cycles for a composite with 10 vol.% nickel filaments. The strain amplitude was 5% under tension and 1.8% under compression. The behavior is similar to that in figure 3 for a composite with 7 vol.% filaments.

In general, the cycle number at which the $\Delta R/R_0$ amplitude started to decrease varied from sample to sample, even for a fixed filament volume fraction and fixed strain amplitudes. However, the behavior of (i) increasing $\Delta R/R_0$ amplitude with cycle number at small numbers of cycles, (ii) decreasing $\Delta R/R_0$ amplitude with cycle number at large numbers of cycles, (iii) increasing values of minimum and maximum $\Delta R/R_0$ with cycle number for essentially all cycle numbers and (iv) leveling off of all the changes at large numbers of cycles was the same for all samples, irrespective of the filament volume fraction and strain amplitudes.

Table 1 shows the variation of the amplitude of $\Delta R/R_0$ with cycle number, strain amplitudes and filament volume fraction. Although both tensile and compressive strain amplitudes varied, the variation of the former was more significant than that of the latter, particularly in the cases of the tensile strain amplitudes being 1 and 5%. The amplitude of $\Delta R/R_0$ increased with tensile strain amplitude at a fixed cycle number and a fixed filament volume fraction, probably because the degree of filament alignment increased with increasing tensile strain amplitude. Moreover, it increased from the first cycle to the tenth cycle when the tensile strain amplitude was 5 or 20%, but decreased when the tensile strain amplitude was 1%. At a fixed tensile strain amplitude of 5%, the $\Delta R/R_0$ amplitude decreased when the filament volume fraction was increased from 7 to 10%. Table 2 shows the corresponding variation of the minimum value of $\Delta R/R_0$ in a cycle. The minimum $\Delta R/R_0$ becomes less negative (or more positive) as cycling progressed, as also shown in figures 3 and 4, due to filament–matrix interface degradation. The minimum $\Delta R/R_0$ became more negative as the tensile strain amplitude increased at a fixed cycle number and a fixed filament volume fraction.

Figure 6 shows the variation of the volume electrical resistivity under no load with filament volume fraction for samples that had never been loaded. The resistivity decreased sharply with increasing filament volume fraction for filament volume fractions from 3 to 7%. At filament volume fractions greater than 7%, the resistivity decreased gradually with increasing filament volume fraction. Thus, the percolation threshold was roughly 5%. The variation of the $\Delta R/R_0$ amplitude with the filament volume fraction (table 1) is probably related to the proximity of 7 vol.% to the percolation threshold. Proximity to the percolation threshold probably helped increase the $\Delta R/R_0$ amplitude.

Because the $\Delta R/R_0$ amplitude varied with cycle number such that it became small at large cycle numbers, the electromechanical effect is of limited use for sensing

Table 1. $\Delta R/R_0$ amplitude for various strain amplitudes, cycle numbers and filament volume fractions.

Strain (%)		$\Delta R/R_0$ amplitude 7 vol.% filaments		Strain (%)		$\Delta R/R_0$ amplitude 10 vol.% filaments	
Tensile	Compressive	1st cycle	10th cycle	Tensile	Compressive	1st cycle	10th cycle
1	0.3	0.11	0.04	—	—	—	—
5	0.2	0.47	0.71	5	1.8	0.27	0.37
20	5	0.69	2.8	—	—	—	—

Table 2. Minimum $\Delta R/R_0$ for various strain amplitudes, cycle numbers and filament volume fractions.

Strain (%)		Minimum $\Delta R/R_0$ 7 vol.% filaments		Strain (%)		Minimum $\Delta R/R_0$ 10 vol.% filaments	
Tensile	Compressive	1st cycle	10th cycle	Tensile	Compressive	1st cycle	10th cycle
1	0.3	−0.11	0.006	—	—	—	—
5	0.2	−0.47	0.51	5	1.8	−0.27	−0.09
20	5	−0.69	−0.43	—	—	—	—

Table 3. Tensile properties of nickel-filament silicone-matrix composites.

Filler vol.%	Ultimate strength (MPa)	Young's modulus (MPa)	Strain at break (%)
0[a]	5.3 ± 1.1	5.3 ± 0.3	105.6 ± 9.4
3[a]	3.9 ± 0.2	4.1 ± 0.1	88.1 ± 2.1
7[a]	4.5 ± 0.5	17.3 ± 0.9	32.8 ± 0.5
10[b]	5.0 ± 0.6	44.7 ± 7.2	18.8 ± 1.2
13[c]	5.4 ± 0.1	67.6 ± 4.5	21.2 ± 2.2
19[c]	5.0 ± 0.3	116.2 ± 22.2	7.4 ± 0.6

[a] Strain rate, 500 mm min^{-1}.
[b] Strain rate, 50 mm min^{-1}.
[c] Strain rate, 5 mm min^{-1}.

in practice, at least in the case of the composites of this paper. However, a different choice of filler may decrease the tendency for filler–matrix interface degradation, so that further development may lead to a practical sensor.

The tensile properties of the composites (based on three samples for each filament volume fraction) are shown in table 3. The ultimate strength was not much affected by the filament addition, whereas the Young's modulus increased and the strain at break decreased with increasing filament volume fraction. These mechanical properties are acceptable for application of these composites (particularly those with 7 and 10 vol.% nickel filaments) as strain sensors.

4. Conclusion

A new electromechanical effect in which the volume electrical resistivity decreased upon tensile loading and increased upon unloading was observed in nickel-filament (randomly oriented and discontinuous) silicone-matrix composites. The effect is probably due to the increase in filament alignment upon tensile loading. It allows tensile strain sensing. However, filament–matrix interface degradation caused the resistivity to increase and the electromechanical effect to diminish as tensile strain cycling progressed beyond the first 10–30 cycles.

References

[1] Pramanik P K, Khastgir D, De S K and Saha T N 1990 *J. Mater. Sci.* **25** 3848–53
[2] Wang X and Chung D D L *Smart Mater. Struct.* at press
[3] Radhakrishnan S, Chakne S and Shelke P N 1994 *Mater. Lett.* **18** 358–62
[4] Kost J, Narkis M and Foux A 1984 *J. Appl. Polym. Sci.* **29** 3937–46
[5] Shui Xiaoping and Chung D D L 1995 *J. Electron. Mater.* **24** 107–13